

Solid-State Nuclear Magnetic Resonance of Triple-Cation Mixed-Halide Perovskites

Noemi Landi, Elena Maurina, Daniela Marongiu, Angelica Simbula, Silvia Borsacchi,* Lucia Calucci, Michele Saba, Elisa Carignani,* and Marco Geppi



Cite This: *J. Phys. Chem. Lett.* 2022, 13, 9517–9525



Read Online

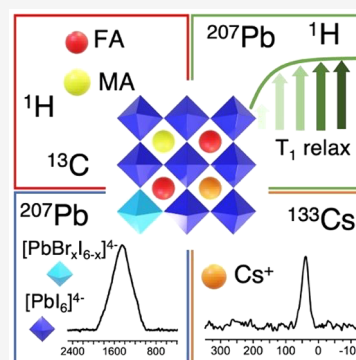
ACCESS |

Metrics & More

Article Recommendations

Supporting Information

ABSTRACT: Mixed-cation lead mixed-halide perovskites are the best candidates for perovskite-based photovoltaics, thanks to their higher efficiency and stability compared to the single-cation single-halide parent compounds. TripleMix ($\text{Cs}_{0.05}\text{MA}_{0.14}\text{FA}_{0.81}\text{PbI}_{2.55}\text{Br}_{0.45}$ with FA = formamidinium and MA = methylammonium) is one of the most efficient and stable mixed perovskites for single-junction solar cells. The microscopic reasons why triple-cation perovskites perform so well are still under debate. In this work, we investigated the structure and dynamics of TripleMix by exploiting multinuclear solid-state nuclear magnetic resonance (SSNMR), which can provide this information at a level of detail not accessible by other techniques. ^{133}Cs , ^{13}C , ^1H , and ^{207}Pb SSNMR spectra confirmed the inclusion of all ions in the perovskite, without phase segregation. Complementary measurements showed a peculiar longitudinal relaxation behavior for the ^1H and ^{207}Pb nuclei in TripleMix with respect to single-cation single-halide perovskites, suggesting slower dynamics of both organic cations and halide anions, possibly related to the high photovoltaic performances.



Hybrid organic–inorganic perovskites are very promising energy materials first reported as active layers in solar cells in 2009¹ and now employed in solar cells exceeding 25% efficiency and even approaching 30% in tandem configuration with silicon.² Perovskites have general formula ABX_3 , and the ideal crystal structure, often distorted, consists of a cube defined by eight corner-sharing $[\text{BX}_6]^{4-}$ octahedra, with the A^+ cation sitting in the center of the cube (Figure 1a). Hybrid lead halide perovskites have an organic cation (or a mix of organic cations) and Pb^{2+} as A^+ and B^{2+} cations, respectively, and the halide (X^-) can be Cl^- , Br^- , I^- .

Attractive features of perovskites include high optical absorption coefficients, long carrier diffusion lengths and lifetimes, small exciton binding energies, high photovoltaic performance, and, especially, the possibility of tuning their optoelectronic properties by changing the stoichiometry and microstructure.³ Over the past decade, Perovskite Solar Cells (PSCs) have reached very high Power Conversion Efficiency (PCE), comparable to that of silicon-based ones.^{2,4} However, issues, arising from structural instabilities and/or the inherent instability in air of the organic cations present in hybrid perovskites, hinder practical applications and commercialization of PSCs.^{5,6} Despite their limitations, metal-halide perovskites are considered exceptional candidates for photovoltaic (PV) applications. Indeed, there is currently substantial interest and ongoing research efforts in developing stabilization strategies for PSCs. In the past few years, it has been found that such stabilization can be achieved, for example, by including different A-site cations and mixing halides into perovskite compositions. To date, perovskites containing a

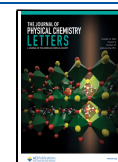
mixture of formamidinium (FA), methylammonium (MA), and cesium (Cs^+) as monovalent cations and a mixture of bromide and iodide as anions are among the best-performing PSCs.^{7–9}

From a structural point of view, a change in the shape and relative orientation of the $[\text{BX}_6]^{4-}$ octahedra (Figure 1a) can lead to modifications of stability, polymorphism, and optical properties of perovskites. The Goldschmidt tolerance factor¹⁰ (t) can be used to predict which phase will form on the basis of the ionic radii of the A^+ , B^{2+} , and X^- ions ($t = (r_{\text{A}} + r_{\text{X}}) / [\sqrt{2}(r_{\text{B}} + r_{\text{X}})]$). Perovskites with a tolerance factor of 0.9–1.0 have an ideal cubic structure, while t values between 0.71 and 0.9 result in a distorted perovskite structure with tilted octahedra.¹¹ The only A-site cations that are known to allow the formation of cubic perovskite structures are MA, FA, and Cs^+ . Na^+ , K^+ , and Rb^+ cations are too small, and organic cations such as ethylammonium, ethylenediaminium, and guanidinium are too large to form a cubic structure on their own, but they can all be used as additives for phase stabilization and defects passivation.¹² In fact, even though MA, FA, and Cs^+ have the ability to form cubic structures, pure MAPbI_3 , FAPbI_3 , and CsPbI_3 present some limitations to their

Received: July 26, 2022

Accepted: September 15, 2022

Published: October 6, 2022



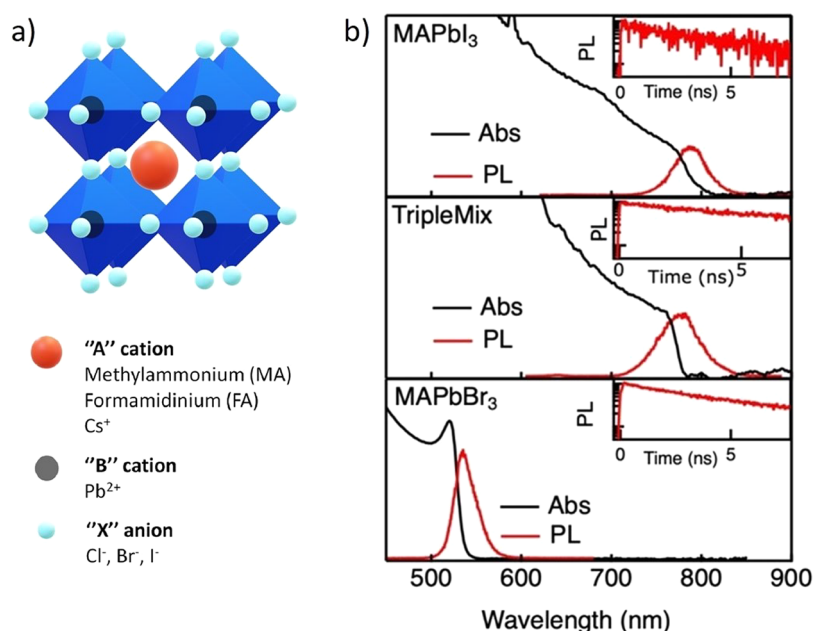


Figure 1. (a) Representation of cubic perovskite structure: eight corner-sharing $[BX_6]^{4-}$ octahedra (blue) forming a cube at the center of which the A^+ cation (orange) lies. (b) Absorption and photoluminescence spectra of $MAPbI_3$, TripleMix, and $MAPbBr_3$. (insets) Photoluminescence decays with time.

practical use in solar devices: (i) $MAPbI_3$ decomposes into methylammonium iodide and PbI_2 under external stimuli (e.g., humidity, temperature);^{13,14} (ii) $FAPbI_3$ has a lower band gap than $MAPbI_3$, resulting in a higher efficiency, but its photoactive perovskite α -phase ("black phase", α - $FAPbI_3$) transforms into the undesirable photoinactive, nonperovskite δ -phase ("yellow phase", δ - $FAPbI_3$) at ambient conditions;^{15,16} (iii) $CsPbI_3$ is stable in the desired photoactive cubic phase only at temperatures above 300 °C, while at room temperature it converts into the photoinactive δ -phase (δ - $CsPbI_3$).⁷ The perovskite phases of $CsPbI_3$ and $FAPbI_3$ are structurally unstable because Cs^+ and FA cations are, respectively, smaller and larger than MA and do not optimally occupy the A-site.¹⁷

Compositional engineering strategies have been extensively explored to overcome the stability issues while pushing the efficiencies higher and higher. By mixing MA and FA cations, better PV performances can be obtained;^{18,19} the addition of MA stabilizes the photoactive phase of $FAPbI_3$, and the charge transport properties improve.²⁰ However, even in the presence of MA, traces of the yellow phase may still form, affecting the crystal morphology and, consequently, the performance.⁷ Moreover, it has been suggested that substituting a small amount of I^- with the smaller Br^- would improve the perovskite stability.^{21,22} However, I^- and Br^- mixing can result in a partial phase segregation when their amounts are nearly equivalent, and this is detrimental to the PSC performance and stability; therefore, attention must be paid to the I^-/Br^- ratio.³

Saliba and co-workers added Cs^+ as a stabilizer to MA/FA mixed perovskites and developed the first solar cells based on a $Cs^+/MA/FA$ mixed cation perovskite with mixed halides, obtaining high performances and improved stability.^{7,23} In fact, even a small amount of Cs^+ is sufficient to effectively suppress the yellow phase of $FAPbI_3$ and induce the formation of highly uniform perovskite grains. The beneficial effects of the addition of Cs^+ to perovskites were investigated and demonstrated also by Zhang et al.²⁴

As mentioned, perovskite compositional flexibility is ideal to tune materials' properties. However, understanding the relationships between composition, properties, and performance is still a challenge. Given the complexity and the broad compositional and structural variety of these materials, this issue can only be addressed by a multidisciplinary approach. In particular, in addition to functionality studies (e.g., studies focused on the synthesis routes and the measurement of optical properties), detailed characterizations of the perovskite structural features and ion dynamics are essential. Techniques typically used to study perovskites are mostly X-ray/electron/neutron diffraction, UV-vis absorption, and photoluminescence (PL) spectroscopies. Recently, it emerged that crucial information on these compounds can be obtained by means of Solid-State Nuclear Magnetic Resonance (SSNMR) spectroscopy, which proved to be very effective in highlighting aspects such as cation incorporation, phase segregation, halide mixing, decomposition mechanisms, disorder, and dynamics, as summarized in recent reviews.^{25–29} The advantage of SSNMR substantially arises from the possibility of observing many different NMR-active isotopes, each having several spin properties sensitive to the atom environment as well as to interactions and dynamics.

SSNMR has proven to be extremely useful for the study of mixed perovskites. For instance, it has been employed to investigate halogens mixing in solid solutions of Cl/Br and Br/I Lead Halide Perovskites (LHPs) of general formula $MAPbX_3$ ³⁰ and $FAPbX_3$,³¹ focusing on the miscibility, phase segregation, and local environments of Pb nuclei. Moreover, the effect of A-cations mixing has been studied by SSNMR in $MA_xFA_{1-x}PbI_3$ ^{32,33} and $Cs_xFA_{1-x}PbBr_3$ ³⁴ double-cation mixed perovskites. In addition to phase segregation, the dynamics of FA and MA was investigated in the latter samples. While no differences in the dynamic behavior were found in $MA_xFA_{1-x}PbI_3$ with respect to the parent pure perovskites, in the case of $Cs_xFA_{1-x}PbBr_3$ the FA dynamics and phase transitions were affected by the presence of Cs^+ . Increasing the

complexity of the systems, the incorporation of Cs⁺, Rb⁺, and K⁺ in MA_xFA_{1-x}PbI₃ was investigated by SSNMR in double-, triple-, and quadrupole-cation perovskites,³⁵ while the only two reports on double/triple-cations and double-halide perovskites by SSNMR concern MA_{0.15}FA_{0.85}PbI_{2.55}Br_{0.45}³³ and Cs_{0.05}MA_{0.16}FA_{0.79}PbI_{2.49}Br_{0.51}.³⁶

In this article, we applied for the first time multinuclear—¹³³Cs, ¹³C, ¹H, ²⁰⁷Pb—SSNMR experiments for the characterization of the triple-cation lead mixed-halide perovskite with formula Cs_{0.05}MA_{0.14}FA_{0.81}PbI_{2.55}Br_{0.45} (in the following indicated as TripleMix), which was found to be in one of the most efficient stoichiometries for single-junction solar cells.⁷ In this SSNMR investigation, we exploited several nuclear probes, complementing spectroscopy experiments with the measurement of nuclear relaxation times, with the aim of highlighting structural and dynamic features related to TripleMix specific stoichiometry.

TripleMix was prepared following the procedure described in the Supporting Information, based on a previously reported synthesis.³⁷ Powder X-ray diffraction (PXRD, Figure S1) confirmed the obtainment of a single perovskite tetragonal phase. MAPbI₃ and MAPbBr₃ parent compounds were also prepared (see Supporting Information) with the aim of analyzing them by means of ²⁰⁷Pb SSNMR and comparing the results with those of TripleMix. Optical characterization, including UV–vis absorption, PL, and Time-Resolved Photoluminescence (TRPL) measurements, was performed on thin films typically used in devices (conditions are detailed in Supporting Information); the results are shown in Figure 1b. MAPbI₃ thin films have a band gap in the near-infrared spectrum, as shown by the onset of the UV–vis absorption at 780 nm. PL is resonant with the band gap, with very limited Stokes shift and few tens of nanometers in width. The trend of PL under femtosecond pulsed excitation, measured with a streak camera, shows a characteristic decay time of several nanoseconds, limited by defects and traps. The time decays become progressively shorter for growing laser fluences, due to the bimolecular nature of carrier recombination in perovskites.³⁸ TripleMix films show very similar optical properties, with a longer PL decay time, due to the reduced nonradiative recombination rate.³⁹ MAPbBr₃ films, instead, have a band gap significantly blue-shifted, due to the effect of the smaller halide radius.

Insights into the structure and dynamics of TripleMix were obtained by SSNMR looking at all present cations through NMR-active nuclei. Starting from A⁺ cations, ¹³³Cs SSNMR can give information on cesium doping ions, known to play a crucial role in perovskite performance and stability. ¹³³Cs is a quadrupolar nucleus ($I = 7/2$), and its high NMR receptivity allows experiments to be carried out even on samples with a very small amount of cesium, like TripleMix. Moreover, the chemical shift of ¹³³Cs ($\delta(^{133}\text{Cs})$) is highly sensitive to its local environment. The ¹³³Cs Magic Angle Spinning (MAS) spectrum of TripleMix (Figure 2a) shows a single signal centered at ca. 37 ppm, with a Full Width at Half-Maximum (fwhm) of about 1.5 kHz. $\delta(^{133}\text{Cs})$, reported in the literature for different perovskites (Table 1), shows a remarkable sensitivity to tiny variations in sample composition. Indeed, in single-cation single-anion perovskites, by changing the halogen, $\delta(^{133}\text{Cs})$ varies from 77 ppm in CsPbCl₃ to 110 and 167 ppm in CsPbBr₃ and γ -CsPbI₃, respectively.⁴⁰ When cesium is introduced in hybrid perovskites, $\delta(^{133}\text{Cs})$ strongly decreases: values from 26 to 50 ppm are reported for $\delta(^{133}\text{Cs})$

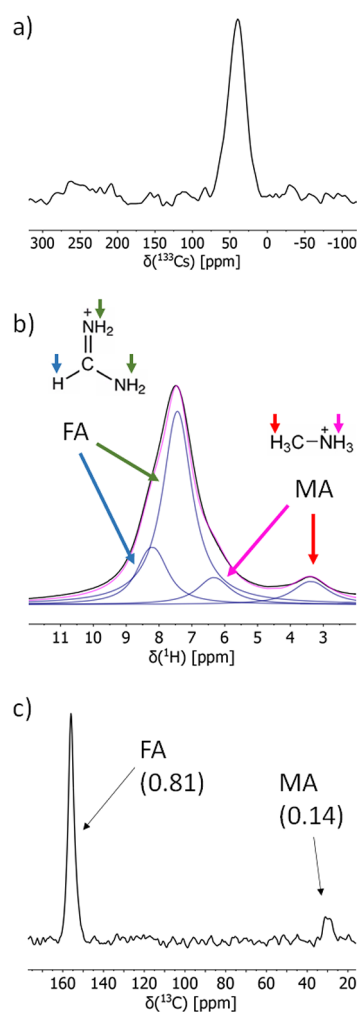


Figure 2. ¹³³Cs (a), ¹H (b), and ¹³C (c) MAS NMR spectra of TripleMix. (b, c) Signal assignments to MA and FA hydrogen and carbon nuclei are also indicated. (c) The relative molar amounts of MA and FA expected for TripleMix are shown in parentheses.

Table 1. ¹³³Cs Chemical Shift Values, $\delta(^{133}\text{Cs})$, of TripleMix and Other Cs-Containing Perovskites Reported in the Literature^{35,36,40}

perovskite	$\delta(^{133}\text{Cs})$, ppm
Cs _{0.05} MA _{0.14} FA _{0.81} PbI _{2.55} Br _{0.45} (TripleMix this work)	37
Cs _{0.05} MA _{0.16} FA _{0.79} PbI _{2.49} Br _{0.51}	~44 ^{36a}
CsPbBr ₃	110 ⁴⁰
γ -CsPbI ₃	167 ⁴⁰
Cs _x FA _{1-x} PbI ₃	
($x = 0.10$)	26, ^{35a}
($x = 0.15$)	31
($x = 0.20$)	39
($x = 0.30$)	50

^aThese $\delta(^{133}\text{Cs})$ values were shifted by +13 ppm with respect to those reported in refs 35 and 36 to be consistent with the IUPAC convention here used for the ¹³³Cs reference.

in Cs_xFA_{1-x}PbI₃ with x ranging from 0.1 to 0.3.³⁵ The value of 37 ppm, here measured for TripleMix, allows us to rule out the presence of CsPbX₃ phases and to assess the full incorporation of Cs⁺ in the mixed perovskite phase. It is interesting to observe that $\delta(^{133}\text{Cs})$ is also sensitive to the presence and amount of MA, as evinced by comparing the value determined

for TripleMix with those, quite different, found for $\text{Cs}_x\text{FA}_{1-x}\text{PbI}_3$ and that of 44 ppm recently reported for a perovskite with chemical formula $\text{Cs}_{0.05}\text{MA}_{0.16}\text{FA}_{0.79}\text{PbI}_{2.49}\text{Br}_{0.51}$.³⁶ The line width of the ^{133}Cs signal in the MAS spectrum of TripleMix (fwhm ≈ 1.5 kHz) is similar to that observed for the other mixed perovskites,^{34–36} while in the spectra of pure CsPbBr_3 and CsPbI_3 phases the ^{133}Cs signal is much narrower (fwhm ≈ 200 –400 Hz).⁴⁰ This finding suggests that, in the mixed samples, a distribution of shifts can arise from slightly different ^{133}Cs environments. Moreover, a reduction of symmetry with respect to that of pure cubic phases can occur in the Cs environment in mixed cation and anion samples, and the line width can consequently be broadened due to quadrupolar coupling. We also recorded ^{133}Cs Rotor-synchronized Hahn-echo experiments at different MAS frequencies (Figure S3b,c), which showed spinning sidebands, in agreement with the static spectrum (Figure S3a).

As far as organic cations are concerned, ^1H and ^{13}C MAS spectra of TripleMix (Figure 2b and c) show the signals of MA and FA and allow a quantification of the FA:MA ratio. This information is not easily obtainable from other techniques, and ^1H SSNMR has been previously proposed as a method of choice for measuring the FA:MA ratio.²⁸ The ^1H MAS spectrum shows two quite broad peaks: a weak one centered at about 3.4 ppm and one, much more intense, centered at about 7.5 ppm. The peak at 3.4 ppm can be straightforwardly ascribed to the sole MA methyl protons, whereas the peak at 7.5 ppm must include the signals of the remaining ^1H nuclei from both MA and FA cations. This becomes clearer by performing a spectral fitting (Figure 2b), which reveals that the signal at higher chemical shift is indeed constituted by three signals at 6.3, 7.4, and 8.2 ppm, which can be assigned to NH_3 of MA, and NH_2 and CH of FA, respectively. The chemical shift values are in agreement with those reported for pure parent perovskites (MAPbI_3 , FAPbI_3) and it has been already reported that they do not significantly change in double-cation compositions^{32,33} and in a triple-cation double-halide perovskite with stoichiometry slightly different from that of TripleMix.³⁶ The signal areas found by spectral fitting were used to quantify the FA:MA ratio, obtaining a ratio of 0.80:0.15 mol:mol, in good agreement with that expected for TripleMix based on the precursors' (MABr and FAI) stoichiometry used in the synthesis (0.81:0.14 mol:mol).

The ^{13}C Direct Excitation (DE) MAS spectrum of TripleMix (Figure 2c) shows one intense signal at 156.0 ppm arising from the CH group of FA and one weak signal at 29.9 ppm for the CH_3 group of MA. The observed chemical shifts are quite similar to those reported for mixed MA/FAPbI₃ perovskites,³² indicating that they are not affected by the presence of Cs^+ and Br^- . Since the spectrum is recorded in quantitative conditions, ensured by a recycle delay between consecutive transients of 75 s, it is possible to obtain a second check for the FA:MA ratio (Figure 2c), which results to be 0.81:0.14 mol:mol.

^1H nuclei can be excellent probes also to investigate the dynamics of FA and MA ions, which has been shown to be related to PV performance.^{41–44} To this aim, proton longitudinal relaxation times, $T_1(^1\text{H})$, were measured at room temperature (RT) at two different Larmor frequencies on TripleMix; the obtained values are reported in Table 2, together with literature data on different perovskites. A single T_1 value is measured at both frequencies, as also reported for other mixed cation perovskites.^{32,33} The fact that all ^1H nuclei

Table 2. $T_1(^1\text{H})$ Values of TripleMix and Other Perovskites (Taken from the Literature) Measured at Room Temperature

perovskite	^1H Larmor frequency	$T_1(^1\text{H})$, s
TripleMix (this work)	400 MHz	16 ± 0.5
	500 MHz	18 ± 0.5
MAPbBr_3	400 MHz	18^{46}
	20 MHz	ca. $18^{47,48}$
MAPbI_3	400 MHz	16^{49}
	400 MHz	15^{50}
	20 MHz	14^{51}
$\text{FA}_{0.67}\text{MA}_{0.33}\text{PbI}_3$	500 MHz	26^{32}
FAPbBr_3	700 MHz	ca. 29^{34}
$\text{Cs}_{0.05}\text{FA}_{0.95}\text{PbBr}_3$	700 MHz	ca. 23^{34}
$\alpha\text{-FAPbI}_3$	500 MHz	33^{48}

show a single T_1 value is a further evidence that a single phase forms, without segregation of different phases. Indeed, if MA and FA would separate in different phases, two different T_1 's could be expected (see Table 2 for $T_1(^1\text{H})$ values of parent perovskites). On the contrary, if organic cations are intimately mixed in a single perovskite phase, spin-diffusion, a diffusion of longitudinal magnetization occurring through homonuclear ^1H – ^1H dipolar couplings, averages different intrinsic T_1 's to a single value.⁴⁵

The dynamics of organic cations in LHPs has been extensively investigated by SSNMR. Early studies on MAPbX_3 , with $\text{X}^- = \text{Cl}^-$, Br^- , I^- , via ^1H , ^2H , and ^{14}N SSNMR spectroscopy,^{47,52,53} showed that MA cations are subjected to a rapid reorientation of the C–N axis at RT, in addition to a very fast rotation along the C–N axis. In recent years, the interest in perovskites for solar cell applications drove a new series of SSNMR studies, which confirmed that, in these perovskites, MA cations undergo a fast jump-like reorientation of the C–N axis at RT.⁴⁹ In the case of MAPbI_3 , a line-shape analysis of ^2H and ^{14}N NMR spectra also allowed the motion geometry to be described in detail and the correlation times to be determined.⁵⁴ Fabiani et al. investigated the dynamics of the FA cation in FAPbI_3 , concluding that its correlation time at RT is comparable to that of MA but the activation energy is much lower.⁴⁸ Kubicki et al. used variable-temperature ^1H , ^2H , ^{13}C , and ^{14}N SSNMR spectroscopy to elucidate the dynamics of the MA and FA cations in pure (MAPbI_3 and FAPbI_3) and mixed cation ($\text{FA}_{0.67}\text{MA}_{0.33}\text{PbI}_3$) perovskites. They concluded that FA reorients faster than MA at RT, but they found no significant differences in the dynamics of both MA and FA in the mixed cation perovskite with respect to the pure reference compounds.³² In addition, Mozur et al. investigated the FA dynamics in Cs-doped FAPbBr_3 , concluding that the crystal distortion introduced by doping disrupts the concerted motions of FA cations at low temperature.³⁴

With respect to the perovskites studied in the previously cited literature, TripleMix represents a step forward in the composition complexity, and this is the first time in which $T_1(^1\text{H})$ values are reported for MA and FA coexisting with Cs, I, and Br in the same lead perovskite. Although a full characterization of the dynamics of organic cations in TripleMix is out of the scope of this work, $T_1(^1\text{H})$ values measured at RT give us some hints. $T_1(^1\text{H})$ values reported for several parent perovskites (Table 2) turned out to be independent of the Larmor frequency at RT or above. From

a first comparison, we can notice that $T_1(^1\text{H})$ of TripleMix is very similar to the lowest values reported in Table 2, thus suggesting that it cannot represent an average of the $T_1(^1\text{H})$ values of the parent compounds. To verify this hypothesis, we calculate an average relaxation time as the inverse of the Population Weighted Relaxation Average (PWRA),^{55,56} expressed by the following equation

$$\text{PWRA} = \langle 1/T_1 \rangle = \frac{x_{\text{FAPbI}_3}}{T_1^{\text{FAPbI}_3}} + \frac{x_{\text{FAPbBr}_3}}{T_1^{\text{FAPbBr}_3}} + \frac{x_{\text{MAPbI}_3}}{T_1^{\text{MAPbI}_3}} + \frac{x_{\text{MAPbBr}_3}}{T_1^{\text{MAPbBr}_3}}$$

under the assumption that the intrinsic $T_1(^1\text{H})$ of MA and FA does not change when passing from parent compounds to TripleMix and neglecting the possible effect of Cs^+ . Using T_1 values reported in Table 2 for the pure parent perovskites and calculating the proton molar fractions (x_i) from the general formula of TripleMix, we obtain $1/\text{PWRA} = 26$ s. Even considering all the approximations, the calculated value is quite larger than the experimental one, thus suggesting a change in the dynamics of organic cations in TripleMix with respect to parent compounds FAPbI₃, FAPbBr₃, MAPbI₃, and MAPbBr₃. This effect, not observed in the case of the mixed sample $\text{FA}_{0.67}\text{MA}_{0.33}\text{PbI}_3$,³² could be related to the presence of a small amount of Cs^+ , as reported for FA in $\text{Cs}_x\text{FA}_{1-x}\text{PbBr}_3$.³⁴ In particular, Cs^+ could induce distortions in the octahedra cavities, which could result in a slowdown of the dynamics of FA and MA. This effect was indeed found by Ghosh et al.⁵⁷ in $\text{Cs}_x\text{FA}_{1-x}\text{PbI}_3$ through ab initio simulations. The computational study showed that the incorporation of Cs^+ cations induces significant structural distortions and that motions of FA cations are significantly inhibited in the mixed samples with respect to FAPbI₃.

To obtain information on the inorganic framework of TripleMix we exploited the SSNMR observation of ²⁰⁷Pb nuclei. Interesting information was obtained from the ²⁰⁷Pb static spectrum of TripleMix, which shows a single very broad signal centered at about 1490 ppm, with fwhm of 34.9 kHz (Figure 3). It is worth noticing that no other signals are observed (even in spectra registered with frequency-stepped acquisition⁵⁸), which confirms the formation of a single phase and excludes the presence of pure parent perovskites and/or PbI_2 that may arise from degradation.

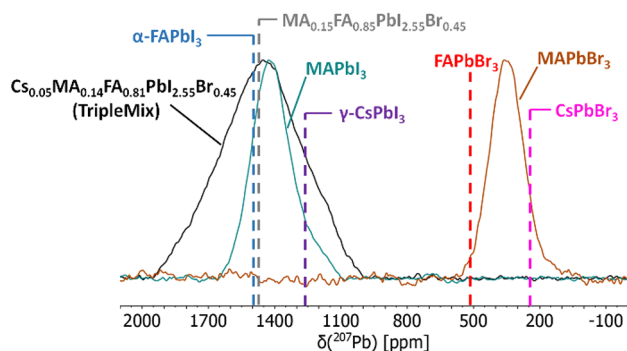


Figure 3. Static ²⁰⁷Pb SSNMR spectra of TripleMix (black) and of the parent perovskites MAPbI₃ (green) and MAPbBr₃ (brown). Dashed lines indicate ²⁰⁷Pb chemical shifts in α -FAPbI₃ (blue), FAPbBr₃ (red), γ -CsPbI₃ (purple), CsPbBr₃ (pink), and $\text{MA}_{0.15}\text{FA}_{0.85}\text{PbI}_{2.55}\text{Br}_{0.45}$ (gray) taken from the literature^{31,33,59} (see Table 3).

Literature data on APbX₃ perovskites (see Table 3) indicate that both the halide and the A⁺ cation affect the ²⁰⁷Pb chemical

Table 3. Chemical Shift, δ , Line Width (fwhm), and T_1 of ²⁰⁷Pb in MAPbBr₃, MAPbI₃, and TripleMix (Measured in This Work) Compared with Those of Other Relevant Perovskites Taken from the Literature. All T_1 Values Were Measured in Static Conditions

perovskite	δ (²⁰⁷ Pb), ppm	fwhm, kHz	T_1 , s
MAPbBr ₃ (this work)	361	14.9	1.54 ± 0.10^a $1.54^{a,60}$
MAPbI ₃ (this work)	1423	17.3	1.32 ± 0.10^a $1.07^{a,60}$
TripleMix (this work)	1450	34.9	0.75 ± 0.10^a
CsPbBr ₃	244 ⁴⁰	13.8 ⁵⁹	
γ -CsPbI ₃	1265 ⁴⁰	20 ⁵⁹	
FAPbBr ₃	510 ^{30,31}	15 ³¹	$1.85^{b,31}$
α -FAPbI ₃	1495 ^{30,31}	ca. 22–26 ³¹	$1.94^{b,31}$
$\text{MA}_{0.15}\text{FA}_{0.85}\text{PbI}_{2.55}\text{Br}_{0.45}$	ca. 1480 ³³	ca. 33 ³³	
$\text{MA}_{0.25}\text{FA}_{0.75}\text{PbI}_3$	ca. 1460 ³³		
$\text{MA}_{0.5}\text{FA}_{0.5}\text{PbI}_3$	ca. 1450 ³³		
$\text{MA}_{0.75}\text{FA}_{0.25}\text{PbI}_3$	ca. 1440 ³³		

^aMeasured at a magnetic field of 9.4 T. ^bMeasured at a magnetic field of 7.0 T.

shift, $\delta(^{207}\text{Pb})$, but the effect of the halide is much stronger. Indeed, in passing from APbBr₃ to APbI₃ a shift of about +1000 ppm is observed.³¹ On the other hand, $\delta(^{207}\text{Pb})$ of α -FAPbI₃ > $\delta(^{207}\text{Pb})$ of MAPbI₃ > $\delta(^{207}\text{Pb})$ of γ -CsPbI₃ with a maximum variation of about 230 ppm. Rosales et al.⁶⁰ demonstrated a linear dependence of $\delta(^{207}\text{Pb})$ on the molar fraction of halide in MAPbI_{(3-x)Br_x}. A linear dependence can also be found for the FAPbI_{(3-x)Br_x} series (Figure S4), from which a $\delta(^{207}\text{Pb})$ value of about 1254 ppm can be predicted for FAPbBr_{0.45}I_{2.55}. Under the hypothesis that the presence of MA and Cs^+ would further shift the ²⁰⁷Pb signal to a lower chemical shift, the chemical shift value here measured for TripleMix indicates that the effect of triple-ion mixing is more complex than the linear effect expected from the sole halogen mixing. Similar findings were already observed, albeit not discussed, by Grüninger et al.,³³ who reported a slight shift to a higher frequency in passing from $\text{MA}_{0.25}\text{FA}_{0.75}\text{PbI}_3$ to $\text{MA}_{0.15}\text{FA}_{0.85}\text{PbI}_{2.55}\text{Br}_{0.45}$. It is also interesting to notice that the presence of a small amount of cesium in TripleMix determines a slight but significant shift of $\delta(^{207}\text{Pb})$ to lower values with respect to the very similar mixed system $\text{MA}_{0.15}\text{FA}_{0.85}\text{PbI}_{2.55}\text{Br}_{0.45}$ (Table 3).³³

A noticeable effect of the presence of mixed cations and anions is observed on the line width of the ²⁰⁷Pb signal; indeed, the fwhm measured in TripleMix is almost twofold that for MAPbI₃ and MAPbBr₃ (Table 3). Generally, ²⁰⁷Pb signals are broad also in single-cation single-halide perovskites. This is mainly ascribable to ²⁰⁷Pb–X scalar coupling combined with a short spin–spin relaxation time (T_2).^{59,207} The ²⁰⁷Pb spectral line shape has been shown to be very sensitive to the nature of the halide ions, with the line broadening increasing passing from Cl[−] to I[−].³¹ By comparison with similar perovskites with mixed cations³³ and anions,³¹ the line width of the TripleMix ²⁰⁷Pb signal can be ascribed to a chemical shift distribution generated by the random distribution of halide ions surrounding each lead nucleus in the coordination octahedra, with an additional contribution from the ²⁰⁷Pb–X scalar

couplings. Our findings are in agreement with data reported for $\text{MA}_{0.15}\text{FA}_{0.85}\text{PbI}_{2.55}\text{Br}_{0.45}$ ³³ and can therefore confirm that, in this compositional range, cation/anion mixing has the most prominent effect on the ²⁰⁷Pb signal broadening.

Finally, $T_1(^{207}\text{Pb})$ values were measured at RT for TripleMix and parent compounds MAPbI_3 and MAPbBr_3 to get insight into the dynamics of $[\text{PbX}_6]^{4-}$ octahedra. Under MAS conditions, the spin–lattice relaxation of ²⁰⁷Pb nuclei is strongly enhanced by a MAS-induced polarization exchange between halogens and lead nuclei,^{50,60–62} with a reduction of T_1 by more than 1 order of magnitude, which prevents other dynamic information to be obtained. Here, $T_1(^{207}\text{Pb})$ values were measured by saturation recovery experiments combined with the Hahn-echo sequence in static conditions. For all samples, the recovery curve was well-reproduced by a single exponential function; the determined $T_1(^{207}\text{Pb})$ values are reported in Table 3, together with values for FAPbBr_3 and $\alpha\text{-FAPbI}_3$ taken from the literature. By comparing T_1 data, an enhanced ²⁰⁷Pb relaxation is evident in TripleMix with respect to MA- and FA-based parent compounds.

²⁰⁷Pb spin–lattice relaxation is complicated, and no interpretation of $T_1(^{207}\text{Pb})$ values has been reported in the literature for LHPs. In a study on PbI_2 , Taylor et al.⁶³ measured $T_1(^{207}\text{Pb})$ at variable temperature and hypothesized two possible physical models for the interpretation: a Raman-like mechanism or a thermally activated mechanism. The first is a lattice-vibration-based relaxation mechanism previously reported for heavy spin-1/2 nuclei,⁶⁴ which implies a peculiar dependence of T_1 on T ($T_1 \propto T^{-2}$) and no magnetic field dependence. On the other hand, the most common thermally activated mechanism assumes that there is a correlation time that characterizes the modulation of the local magnetic interactions in the surrounding of the ²⁰⁷Pb nuclei. In the case of PbI_2 , the authors supposed that the thermally activated process could be iodine ion hopping (observed by ¹²⁷I T_1), which affects ²⁰⁷Pb relaxation through scalar coupling, but this hypothesis has not been confirmed yet.

Motions of the octahedra in LHPs have been postulated and observed by SSNMR, but a complete understanding is still missing. In particular, from variable-temperature ²⁰⁷Pb T_2 measurements Kentgens and colleagues⁶⁵ concluded that $[\text{PbI}_6]^{4-}$ octahedra in MAPbI_3 are subjected to a slow motion. In addition, Aebli et al. were able to resolve Pb–Br scalar couplings in low-temperature ²⁰⁷Pb SSNMR spectra and ascribed the lower resolution at RT to structural dynamics and/or a degree of disorder in APbBr_3 perovskites (with $\text{A}^+ = \text{Cs}^+$, MA, and FA).⁵⁹ Molecular dynamics simulations of $\text{Cs}_x\text{FA}_{1-x}\text{PbI}_3$ showed that dynamic tilting of $[\text{PbI}_6]^{4-}$ octahedra is inhibited by Cs^+ incorporation.⁵⁷ In addition, halide ion migration has been shown to be slower in $\text{Cs}_{0.3}\text{MA}_{0.7}\text{PbBr}_{1.5}\text{I}_{1.5}$ and $\text{Cs}_{0.5}\text{MA}_{0.5}\text{PbBr}_{1.5}\text{I}_{1.5}$ than in $\text{MAPbBr}_{1.5}\text{I}_{1.5}$.^{66,67} The lower value of $T_1(^{207}\text{Pb})$ measured in this work for TripleMix with respect to pure parent compounds is in agreement with these last results and indicates that dynamic tilting of $[\text{PbX}_6]^{4-}$ octahedra and/or halide mobility are slowed down also in our perovskite.

In conclusion, this is the first multinuclear SSNMR investigation of the very well-performing triple-cation lead double-halide perovskite $\text{Cs}_{0.05}\text{MA}_{0.14}\text{FA}_{0.81}\text{PbI}_{2.55}\text{Br}_{0.45}$, including both recording of spectra and measurements of nuclear spin–lattice relaxation times. From a detailed comparison with data on parent compounds, it emerged that the chemical shift of ²⁰⁷Pb in TripleMix is intermediate between those of FAPbI_3

and MAPbI_3 , while the presence of a small amount of bromine does not lead to a significant decrease of chemical shift, in agreement with data reported for $\text{MA}_{0.15}\text{FA}_{0.85}\text{PbI}_{2.55}\text{Br}_{0.45}$.³³ Moreover, the comparison with $\text{MA}_{0.15}\text{FA}_{0.85}\text{PbI}_{2.55}\text{Br}_{0.45}$ highlighted a decrease of the chemical shift ascribable to the presence of the small amount of cesium. The ²⁰⁷Pb signal line width, larger than that of pure LHPs and comparable to that of $\text{MA}_{0.15}\text{FA}_{0.85}\text{PbI}_{2.55}\text{Br}_{0.45}$, indicated a distribution of Pb coordination environments. Interestingly, the T_1 of ²⁰⁷Pb nuclei was noticeably lower than those of parent pure compounds, suggesting a peculiarly enhanced relaxation related to the mixed composition.

As far as A^+ cations are concerned, ¹H, ¹³C, and ¹³³Cs NMR spectra confirmed the stoichiometry of TripleMix and the effective mixing of the cations, ruling out the occurrence of phase segregation. Similarly to what observed for ²⁰⁷Pb, the ¹H nuclei of the organic cations showed an enhanced spin–lattice relaxation. Indeed, $T_1(^1\text{H})$ values indicated interesting differences in the dynamics of organic cations with respect to pure compounds, suggesting that the mixing induces structural changes that could slow down the reorientational motion of FA and MA, not observed for other mixed-cation perovskites. These results suggest an important role of Cs^+ in altering the dynamic properties of MA and FA, which could be related to the suppression of collective organic and inorganic motions, in turn affecting carrier lifetimes. This hypothesis is supported by a previous computational study⁵⁷ and by the observation of the effect of Cs^+ in altering the concerted cation dynamics in $\text{Cs}_x\text{FA}_{1-x}\text{PbBr}_3$,³⁴ while the correlation between altered dynamics of FA/MA and changes in carrier lifetimes was highlighted by studying the effect of deuteration in MAPbI_3 and FAPbI_3 .^{41–43}

The results obtained in this work encourage us to further investigate the dynamics of cations in complex perovskites by measuring nuclear relaxation times at variable temperature and magnetic field.

■ ASSOCIATED CONTENT

Supporting Information

The Supporting Information is available free of charge at <https://pubs.acs.org/doi/10.1021/acs.jpcllett.2c02313>.

Experimental details, materials, and methods; additional structural and optical properties of TripleMix and parent perovskites; additional ¹³³Cs spectra and details about ²⁰⁷Pb chemical shift analysis (PDF)

■ AUTHOR INFORMATION

Corresponding Authors

Silvia Borsacchi – *Institute for the Chemistry of OrganoMetallic Compounds - ICCOM, Italian National Research Council - CNR, 56124 Pisa, Italy; Center for Instrument Sharing, University of Pisa (CISUP), 56126 Pisa, Italy; orcid.org/0000-0003-3696-0719; Email: silvia.borsacchi@pi.iccom.cnr.it*

Elisa Carignani – *Institute for the Chemistry of OrganoMetallic Compounds - ICCOM, Italian National Research Council - CNR, 56124 Pisa, Italy; orcid.org/0000-0001-5848-9660; Email: elisa.carignani@cnr.it*

Authors

Noemi Landi – *Department of Chemistry and Industrial Chemistry, University of Pisa, 56124 Pisa, Italy*

Elena Maurina – Department of Chemistry and Industrial Chemistry, University of Pisa, 56124 Pisa, Italy; Present Address: Information Engineering Department, University of Pisa, via G. Caruso 16, 56122, Pisa, Italy

Daniela Marongiu – Department of Physics, University of Cagliari, 09042 Monserrato, Cagliari, Italy; orcid.org/0000-0001-7085-769X

Angelica Simbula – Department of Physics, University of Cagliari, 09042 Monserrato, Cagliari, Italy

Lucia Calucci – Institute for the Chemistry of OrganoMetallic Compounds - ICCOM, Italian National Research Council - CNR, 56124 Pisa, Italy; Center for Instrument Sharing, University of Pisa (CISUP), 56126 Pisa, Italy; orcid.org/0000-0002-3080-8807

Michele Saba – Department of Physics, University of Cagliari, 09042 Monserrato, Cagliari, Italy; orcid.org/0000-0001-6416-3122

Marco Geppi – Department of Chemistry and Industrial Chemistry, University of Pisa, 56124 Pisa, Italy; Institute for the Chemistry of OrganoMetallic Compounds - ICCOM, Italian National Research Council - CNR, 56124 Pisa, Italy; Center for Instrument Sharing, University of Pisa (CISUP), 56126 Pisa, Italy; orcid.org/0000-0002-2422-8400

Complete contact information is available at:

<https://pubs.acs.org/10.1021/acs.jpcl.2c02313>

Notes

The authors declare no competing financial interest.

ACKNOWLEDGMENTS

CISUP (Centre for Instrument Sharing—University of Pisa) is acknowledged for the use of the Bruker Avance Neo 500 Solid State NMR Spectrometer. CeSAR—Centro Servizi di Ateneo per la Ricerca—at Università degli Studi di Cagliari is acknowledged for access to research infrastructures for XRD and TRPL. PON “Ricerca e Innovazione” 2014–2020 – Fondo Sociale Europeo, Attraction and International Mobility—AIM1809115-2, Linea 2.1 is acknowledged for financial support.

ABBREVIATIONS

DE, direct excitation; FA, formamidinium; fwhm, full width at half-maximum; LHP, lead halide perovskite; MA, methylammonium; MAS, magic angle spinning; PL, photoluminescence; PSC, perovskite solar cells; PV, photovoltaic; PXRD, powder X-ray diffraction; RT, room temperature; SSNMR, solid state nuclear magnetic resonance; TRPL, time-resolved photoluminescence

REFERENCES

- (1) Kojima, A.; Teshima, K.; Shirai, Y.; Miyasaka, T. Organometal Halide Perovskites as Visible-Light Sensitizers for Photovoltaic Cells. *J. Am. Chem. Soc.* **2009**, *131*, 6050–6051.
- (2) Green, M. A.; Dunlop, E. D.; Hohl-Ebinger, J.; Yoshita, M.; Kopidakis, N.; Hao, X. Solar Cell Efficiency Tables (Version 59). *Prog. Photovolt.: Res. Appl.* **2022**, *30*, 3–12.
- (3) Correa-Baena, J.-P.; Saliba, M.; Buonassisi, T.; Grätzel, M.; Abate, A.; Tress, W.; Hagfeldt, A. Promises and Challenges of Perovskite Solar Cells. *Science* **2017**, *358*, 739–744.
- (4) Basumatary, P.; Agarwal, P. A Short Review on Progress in Perovskite Solar Cells. *Mater. Res. Bull.* **2022**, *149*, 111700.
- (5) Poorkazem, K.; Kelly, T. L. Compositional Engineering to Improve the Stability of Lead Halide Perovskites: A Comparative

Study of Cationic and Anionic Dopants. *ACS Appl. Energy Mater.* **2018**, *1*, 181–190.

(6) Wang, F.; Ma, J.; Xie, F.; Li, L.; Chen, J.; Fan, J.; Zhao, N. Organic Cation-Dependent Degradation Mechanism of Organotin Halide Perovskites. *Adv. Funct. Mater.* **2016**, *26*, 3417–3423.

(7) Saliba, M.; Matsui, T.; Seo, J. Y.; Domanski, K.; Correa-Baena, J. P.; Nazeeruddin, M. K.; Zakeeruddin, S. M.; Tress, W.; Abate, A.; Hagfeldt, A.; Grätzel, M. Cesium-Containing Triple Cation Perovskite Solar Cells: Improved Stability, Reproducibility and High Efficiency. *Energy Environ. Sci.* **2016**, *9*, 1989–1997.

(8) Yang, W. S.; Park, B.-W.; Jung, E. H.; Jeon, N. J.; Kim, Y. C.; Lee, D. U.; Shin, S. S.; Seo, J.; Kim, E. K.; Noh, J. H.; Seok, S. I. Iodide Management in Formamidinium-Lead-Halide-Based Perovskite Layers for Efficient Solar Cells. *Science* **2017**, *356*, 1376–1379.

(9) Lu, H.; Krishna, A.; Zakeeruddin, S. M.; Grätzel, M.; Hagfeldt, A. Compositional and Interface Engineering of Organic-Inorganic Lead Halide Perovskite Solar Cells. *iScience* **2020**, *23*, 101359.

(10) Goldschmidt, V. M. Die Gesetze Der Krystallochemie. *Naturwissenschaften* **1926**, *14*, 477–485.

(11) Li, Z.; Yang, M.; Park, J.-S.; Wei, S.-H.; Berry, J. J.; Zhu, K. Stabilizing Perovskite Structures by Tuning Tolerance Factor: Formation of Formamidinium and Cesium Lead Iodide Solid-State Alloys. *Chem. Mater.* **2016**, *28*, 284–292.

(12) Han, G.; Hadi, H. D.; Bruno, A.; Kulkarni, S. A.; Koh, T. M.; Wong, L. H.; Soci, C.; Mathews, N.; Zhang, S.; Mhaisalkar, S. G. Additive Selection Strategy for High Performance Perovskite Photovoltaics. *J. Phys. Chem. C* **2018**, *122*, 13884–13893.

(13) Askar, A. M.; Bernard, G. M.; Wiltshire, B.; Shankar, K.; Michaelis, V. K. Multinuclear Magnetic Resonance Tracking of Hydro, Thermal, and Hydrothermal Decomposition of $\text{CH}_3\text{NH}_3\text{PbI}_3$. *J. Phys. Chem. C* **2017**, *121*, 1013–1024.

(14) Ciccio, A.; Latini, A. Thermodynamics and the Intrinsic Stability of Lead Halide Perovskites $\text{CH}_3\text{NH}_3\text{PbX}_3$. *J. Phys. Chem. Lett.* **2018**, *9*, 3756–3765.

(15) Eperon, G. E.; Stranks, S. D.; Menelaou, C.; Johnston, M. B.; Herz, L. M.; Snaith, H. J. Formamidinium Lead Trihalide: A Broadly Tunable Perovskite for Efficient Planar Heterojunction Solar Cells. *Energy Environ. Sci.* **2014**, *7*, 982.

(16) Luongo, A.; Brunetti, B.; Vecchio Cipriotti, S.; Ciccio, A.; Latini, A. Thermodynamic and Kinetic Aspects of Formamidinium Lead Iodide Thermal Decomposition. *J. Phys. Chem. C* **2021**, *125*, 21851–21861.

(17) Travis, W.; Glover, E. N. K.; Bronstein, H.; Scanlon, D. O.; Palgrave, R. G. On the Application of the Tolerance Factor to Inorganic and Hybrid Halide Perovskites: A Revised System. *Chem. Sci.* **2016**, *7*, 4548–4556.

(18) Wang, C.; Zhao, D.; Yu, Y.; Shrestha, N.; Grice, C. R.; Liao, W.; Cimaroli, A. J.; Chen, J.; Ellingson, R. J.; Zhao, X.; Yan, Y. Compositional and Morphological Engineering of Mixed Cation Perovskite Films for Highly Efficient Planar and Flexible Solar Cells with Reduced Hysteresis. *Nano Energy* **2017**, *35*, 223–232.

(19) Zhang, Y.; Grancini, G.; Feng, Y.; Asiri, A. M.; Nazeeruddin, M. K. Optimization of Stable Quasi-Cubic $\text{FA}_{1-x}\text{MA}_x\text{PbI}_3$ Perovskite Structure for Solar Cells with Efficiency beyond 20%. *ACS Energy Lett.* **2017**, *2*, 802–806.

(20) Zhu, C.; Niu, X.; Fu, Y.; Li, N.; Hu, C.; Chen, Y.; He, X.; Na, G.; Liu, P.; Zai, H.; Ge, Y.; Lu, Y.; Ke, X.; Bai, Y.; Yang, S.; Chen, P.; Li, Y.; Sui, M.; Zhang, L.; Zhou, H.; Chen, Q. Strain Engineering in Perovskite Solar Cells and Its Impacts on Carrier Dynamics. *Nat. Commun.* **2019**, *10*, 815.

(21) Sutton, R. J.; Eperon, G. E.; Miranda, L.; Parrott, E. S.; Kamino, B. A.; Patel, J. B.; Hörantner, M. T.; Johnston, M. B.; Haghighirad, A. A.; Moore, D. T.; Snaith, H. J. Bandgap-Tunable Cesium Lead Halide Perovskites with High Thermal Stability for Efficient Solar Cells. *Adv. Energy Mater.* **2016**, *6*, 1502458.

(22) Jesper Jacobsson, T.; Correa-Baena, J.-P.; Pazoki, M.; Saliba, M.; Schenk, K.; Grätzel, M.; Hagfeldt, A. Exploration of the Compositional Space for Mixed Lead Halogen Perovskites for High Efficiency Solar Cells. *Energy Environ. Sci.* **2016**, *9*, 1706–1724.

- (23) McMeekin, D. P.; Sadoughi, G.; Rehman, W.; Eperon, G. E.; Saliba, M.; Hörlantner, M. T.; Haghighirad, A.; Sakai, N.; Korte, L.; Rech, B.; Johnston, M. B.; Herz, L. M.; Snaith, H. J. A Mixed-Cation Lead Mixed-Halide Perovskite Absorber for Tandem Solar Cells. *Science* **2016**, *351*, 151–155.
- (24) Zhang, R.; Liu, D.; Wang, Y.; Zhang, T.; Gu, X.; Zhang, P.; Wu, J.; Chen, Z. D.; Zhao, Y.; Li, S. Theoretical Lifetime Extraction and Experimental Demonstration of Stable Cesium-Containing Tri-Cation Perovskite Solar Cells with High Efficiency. *Electrochim. Acta* **2018**, *265*, 98–106.
- (25) Piveteau, L.; Morad, V.; Kovalenko, M. V. Solid-State NMR and NQR Spectroscopy of Lead-Halide Perovskite Materials. *J. Am. Chem. Soc.* **2020**, *142*, 19413–19437.
- (26) Aiello, F.; Masi, S. The Contribution of NMR Spectroscopy in Understanding Perovskite Stabilization Phenomena. *J. Nanomater.* **2021**, *11*, 2024.
- (27) Franssen, W. M. J.; Kentgens, A. P. M. Solid-State NMR of Hybrid Halide Perovskites. *Solid State Nucl. Magn. Reson.* **2019**, *100*, 36–44.
- (28) Kubicki, D. J.; Stranks, S. D.; Grey, C. P.; Emsley, L. NMR Spectroscopy Probes Microstructure, Dynamics and Doping of Metal Halide Perovskites. *Nat. Rev. Chem.* **2021**, *5*, 624–645.
- (29) Quarti, C.; Furet, E.; Katan, C. DFT Simulations as Valuable Tool to Support NMR Characterization of Halide Perovskites: The Case of Pure and Mixed Halide Perovskites. *Helv. Chim. Acta* **2021**, *104* e2000231 DOI: 10.1002/hlca.202000231.
- (30) Karmakar, A.; Askar, A. M.; Bernard, G. M.; Terskikh, V. V.; Ha, M.; Patel, S.; Shankar, K.; Michaelis, V. K. Mechanochemical Synthesis of Methylammonium Lead Mixed-Halide Perovskites: Unraveling the Solid-Solution Behavior Using Solid-State NMR. *Chem. Mater.* **2018**, *30*, 2309–2321.
- (31) Askar, A. M.; Karmakar, A.; Bernard, G. M.; Ha, M.; Terskikh, V. V.; Wiltshire, B. D.; Patel, S.; Fleet, J.; Shankar, K.; Michaelis, V. K. Composition-Tunable Formamidinium Lead Mixed Halide Perovskites via Solvent-Free Mechanochemical Synthesis: Decoding the Pb Environments Using Solid-State NMR Spectroscopy. *J. Phys. Chem. Lett.* **2018**, *9*, 2671–2677.
- (32) Kubicki, D. J.; Prochowicz, D.; Hofstetter, A.; Péchy, P.; Zakeeruddin, S. M.; Grätzel, M.; Emsley, L. Cation Dynamics in Mixed-Cation (MA)_x(FA)_{1-x}PbI₃ Hybrid Perovskites from Solid-State NMR. *J. Am. Chem. Soc.* **2017**, *139*, 10055–10061.
- (33) Grüninger, H.; Bokdam, M.; Leupold, N.; Tinnemans, P.; Moos, R.; de Wijs, G. A.; Panzer, F.; Kentgens, A. P. M. Microscopic (Dis)Order and Dynamics of Cations in Mixed FA/MA Lead Halide Perovskites. *J. Phys. Chem. C* **2021**, *125*, 1742–1753.
- (34) Mozur, E. M.; Hope, M. A.; Trowbridge, J. C.; Halat, D. M.; Daemen, L. L.; Maughan, A. E.; Prisk, T. R.; Grey, C. P.; Neilson, J. R. Cesium Substitution Disrupts Concerted Cation Dynamics in Formamidinium Hybrid Perovskites. *Chem. Mater.* **2020**, *32*, 6266–6277.
- (35) Kubicki, D. J.; Prochowicz, D.; Hofstetter, A.; Zakeeruddin, S. M.; Grätzel, M.; Emsley, L. Phase Segregation in Cs-, Rb- and K-Doped Mixed-Cation (MA)_x(FA)_{1-x}PbI₃ Hybrid Perovskites from Solid-State NMR. *J. Am. Chem. Soc.* **2017**, *139*, 14173–14180.
- (36) Kazemi, M. A. A.; Folastre, N.; Raval, P.; Sliwa, M.; Nsanjimana, J. M. V.; Golon, S.; Demortiere, A.; Rousset, J.; Lafon, O.; Delevoeye, L.; Reddy, G. N. M.; Sauvage, F. Moisture-Induced Non-Equilibrium Phase Segregation in Triple Cation Mixed Halide Perovskite Monitored by In Situ Characterization Techniques and Solid-State NMR. *Energy Environ. Mater.* **2022**, *0*, 1–10, DOI: 10.1002/eem2.12335.
- (37) Tan, H.; Jain, A.; Voznyy, O.; Lan, X.; García de Arquer, F. P.; Fan, J. Z.; Quintero-Bermudez, R.; Yuan, M.; Zhang, B.; Zhao, Y.; Fan, F.; Li, P.; Quan, L. N.; Zhao, Y.; Lu, Z.-H.; Yang, Z.; Hoogland, S.; Sargent, E. H. Efficient and Stable Solution-Processed Planar Perovskite Solar Cells via Contact Passivation. *Science* **2017**, *355*, 722–726.
- (38) Saba, M.; Quochi, F.; Mura, A.; Bongiovanni, G. Excited State Properties of Hybrid Perovskites. *Acc. Chem. Res.* **2016**, *49*, 166–173.
- (39) Simbula, A.; Pau, R.; Liu, F.; Wu, L.; Lai, S.; Geddo-Lehmann, A.; Filippetti, A.; Loi, M. A.; Marongiu, D.; Quochi, F.; Saba, M.; Mura, A.; Bongiovanni, G. Direct Measurement of Radiative Decay Rates in Metal Halide Perovskites. *Energy Environ. Sci.* **2022**, *15*, 1211–1221.
- (40) Karmakar, A.; Dodd, M. S.; Zhang, X.; Oakley, M. S.; Klobukowski, M.; Michaelis, V. K. Mechanochemical Synthesis of 0D and 3D Cesium Lead Mixed Halide Perovskites. *Chem. Commun.* **2019**, *55*, 5079–5082.
- (41) Gong, J.; Yang, M.; Ma, X.; Schaller, R. D.; Liu, G.; Kong, L.; Yang, Y.; Beard, M. C.; Lesslie, M.; Dai, Y.; Huang, B.; Zhu, K.; Xu, T. Electron–Rotor Interaction in Organic–Inorganic Lead Iodide Perovskites Discovered by Isotope Effects. *J. Phys. Chem. Lett.* **2016**, *7*, 2879–2887.
- (42) Zhao, X.; Long, R. Isotopic Exchange Extends Charge Carrier Lifetime in Metal Lead Perovskites by Quantum Dynamics Simulations. *J. Phys. Chem. Lett.* **2020**, *11*, 10298–10305.
- (43) Solanki, A.; Tavakoli, M. M.; Xu, Q.; Dintakurti, S. S. H.; Lim, S. S.; Bagui, A.; Hanna, J. v.; Kong, J.; Sum, T. C. Heavy Water Additive in Formamidinium: A Novel Approach to Enhance Perovskite Solar Cell Efficiency. *Adv. Mater.* **2020**, *32*, 1907864.
- (44) Motta, C.; El-Mellouhi, F.; Kais, S.; Tabet, N.; Alharbi, F.; Sanvito, S. Revealing the Role of Organic Cations in Hybrid Halide Perovskite CH₃NH₃PbI₃. *Nat. Commun.* **2015**, *6*, 7026.
- (45) Müller, K.; Geppi, M. *Solid State NMR: Principles, Methods, and Applications*; Wiley-VCH: Weinheim, Germany, 2021.
- (46) Senocrate, A. *Defect Chemistry of Methylammonium Lead Iodide*; École Polytechnique Fédérale De Lausanne: Switzerland, 2018.
- (47) Xu, Q.; Eguchi, T.; Nakayama, H.; Nakamura, N.; Kishita, M. Molecular Motions and Phase Transitions in Solid CH₃NH₃PbX₃ (X = Cl, Br, I) as Studied by NMR and NQR. *Z. Naturforsch. A* **1991**, *46*, 240–246.
- (48) Fabiani, D. H.; Siaw, T. A.; Stoumpos, C. C.; Laurita, G.; Olds, D.; Page, K.; Hu, J. G.; Kanatzidis, M. G.; Han, S.; Seshadri, R. Universal Dynamics of Molecular Reorientation in Hybrid Lead Iodide Perovskites. *J. Am. Chem. Soc.* **2017**, *139*, 16875–16884.
- (49) Baikie, T.; Barrow, N. S.; Fang, Y.; Keenan, P. J.; Slater, P. R.; Piltz, R. O.; Gutmann, M.; Mhaisalkar, S. G.; White, T. J. A Combined Single Crystal Neutron/X-Ray Diffraction and Solid-State Nuclear Magnetic Resonance Study of the Hybrid Perovskites CH₃NH₃PbX₃ (X = I, Br and Cl). *J. Mater. Chem. A* **2015**, *3*, 9298–9307.
- (50) Senocrate, A.; Moudrakovski, I.; Maier, J. Short-Range Ion Dynamics in Methylammonium Lead Iodide by Multinuclear Solid State NMR and ¹²⁷I NQR. *Phys. Chem. Chem. Phys.* **2018**, *20*, 20043–20055.
- (51) Colella, S.; Todaro, M.; Masi, S.; Listorti, A.; Altamura, D.; Caliendo, R.; Giannini, C.; Carignani, E.; Geppi, M.; Meggiolaro, D.; Buscarino, G.; de Angelis, F.; Rizzo, A. Light-Induced Formation of Pb³⁺ Paramagnetic Species in Lead Halide Perovskites. *ACS Energy Lett.* **2018**, *3*, 1840–1847.
- (52) Wasylshen, R. E.; Knop, O.; Macdonald, J. B. Cation Rotation in Methylammonium Lead Halides. *Solid State Commun.* **1985**, *56*, 581–582.
- (53) Knop, O.; Wasylshen, R. E.; White, M. A.; Cameron, T. S.; Oort, M. J. M. V. Alkylammonium Lead Halides. Part 2. CH₃NH₃PbX₃ (X = Cl, Br, I) Perovskites: Cuboctahedral Halide Cages with Isotropic Cation Reorientation. *Can. J. Chem.* **1990**, *68*, 412–422.
- (54) Bernard, G. M.; Wasylshen, R. E.; Ratcliffe, C. I.; Terskikh, V.; Wu, Q.; Buriak, J. M.; Hauger, T. Methylammonium Cation Dynamics in Methylammonium Lead Halide Perovskites: A Solid-State NMR Perspective. *J. Phys. Chem. A* **2018**, *122*, 1560–1573.
- (55) Kenwright, A. M.; Say, B. J. Analysis of Spin-Diffusion Measurements by Iterative Optimisation of Numerical Models. *Solid State Nucl. Magn. Reson.* **1996**, *7*, 85–93.
- (56) Geppi, M.; Harris, R. K.; Kenwright, A. M.; Say, B. J. A Method for Analysing Proton NMR Relaxation Data from Motionally

Heterogeneous Polymer Systems. *Solid State Nucl. Magn. Reson.* **1998**, *12*, 15–20.

(57) Ghosh, D.; Smith, A. R.; Walker, A. B.; Islam, M. S. Mixed A-Cation Perovskites for Solar Cells: Atomic-Scale Insights into Structural Distortion, Hydrogen Bonding, and Electronic Properties. *Chem. Mater.* **2018**, *30*, 5194–5204.

(58) Pell, A. J.; Clément, R. J.; Grey, C. P.; Emsley, L.; Pintacuda, G. Frequency-Stepped Acquisition in Nuclear Magnetic Resonance Spectroscopy under Magic Angle Spinning. *J. Chem. Phys.* **2013**, *138*, 114201.

(59) Aebli, M.; Piveteau, L.; Nazarenko, O.; Benin, B. M.; Krieg, F.; Verel, R.; Kovalenko, M. V. Lead-Halide Scalar Couplings in ^{207}Pb NMR of APbX_3 Perovskites (A = Cs, Methylammonium, Formamidinium; X = Cl, Br, I). *Sci. Rep.* **2020**, *10*, 8229.

(60) Rosales, B. A.; Men, L.; Cady, S. D.; Hanrahan, M. P.; Rossini, A. J.; Vela, J. Persistent Dopants and Phase Segregation in Organolead Mixed-Halide Perovskites. *Chem. Mater.* **2016**, *28*, 6848–6859.

(61) Lee, J.; Lee, W.; Kang, K.; Lee, T.; Lee, S. K. Layer-by-Layer Structural Identification of 2D Ruddlesden–Popper Hybrid Lead Iodide Perovskites by Solid-State NMR Spectroscopy. *Chem. Mater.* **2021**, *33*, 370–377.

(62) Shmyreva, A. A.; Safdari, M.; Furó, I.; Dvinskikh, S. V. NMR Longitudinal Relaxation Enhancement in Metal Halides by Heteronuclear Polarization Exchange during Magic-Angle Spinning. *J. Chem. Phys.* **2016**, *144*, 224201.

(63) Taylor, R. E.; Beckmann, P. A.; Bai, S.; Dybowski, C. ^{127}I and ^{207}Pb Solid-State NMR Spectroscopy and Nuclear Spin Relaxation in PbI_2 : A Preliminary Study. *J. Phys. Chem. C* **2014**, *118*, 9143–9153.

(64) Vega, A. J.; Beckmann, P. A.; Bai, S.; Dybowski, C. Spin-Lattice Relaxation of Heavy Spin-1/2 Nuclei in Diamagnetic Solids: A Raman Process Mediated by Spin-Rotation Interaction. *Phys. Rev. B* **2006**, *74*, 214420.

(65) Franssen, W. M. J.; van Es, S. G. D.; Dervişoğlu, R.; de Wijs, G. A.; Kentgens, A. P. M. Symmetry, Dynamics, and Defects in Methylammonium Lead Halide Perovskites. *J. Phys. Chem. Lett.* **2017**, *8*, 61–66.

(66) Hutter, E. M.; Muscarella, L. A.; Wittmann, F.; Versluis, J.; McGovern, L.; Bakker, H. J.; Woo, Y.-W.; Jung, Y.-K.; Walsh, A.; Ehrler, B. Thermodynamic Stabilization of Mixed-Halide Perovskites against Phase Segregation. *Cell. Rep. Phys. Sci.* **2020**, *1*, 100120.

(67) Muscarella, L. A.; Hutter, E. M.; Wittmann, F.; Woo, Y. W.; Jung, Y.-K.; McGovern, L.; Versluis, J.; Walsh, A.; Bakker, H. J.; Ehrler, B. Lattice Compression Increases the Activation Barrier for Phase Segregation in Mixed-Halide Perovskites. *ACS Energy Lett.* **2020**, *5*, 3152–3158.

Recommended by ACS

Role of Monovalent Cations in the Dielectric Relaxation Processes in Hybrid Metal Halide Perovskite Solar cells

Kashimul Hossain, Dinesh Kabra, *et al.*

MARCH 17, 2022
ACS APPLIED ENERGY MATERIALS

READ 

Ion-Assisted Ligand Exchange for Efficient and Stable Inverted FAPbI_3 Quantum Dot Solar Cells

Yuanze Xu, Qiuming Yu, *et al.*

AUGUST 05, 2022
ACS APPLIED ENERGY MATERIALS

READ 

A-Site Mixing to Adjust the Photovoltaic Performance of a Double-Cation Perovskite: It Is Not Always the Simple Way

Wen-Cheng Qiao, Ye-Feng Yao, *et al.*

NOVEMBER 11, 2021
THE JOURNAL OF PHYSICAL CHEMISTRY LETTERS

READ 

Hybrid Organic–Inorganic Halide Derivatives of the 2H Hexagonal Perovskite Structure

Noah P. Holzapfel, Patrick M. Woodward, *et al.*

AUGUST 25, 2022
CHEMISTRY OF MATERIALS

READ 

Get More Suggestions >